



# Technische Universität München

Lehrstuhl für Bioverfahrenstechnik

Semesterarbeit

## **Development of a Low-Cost Electrical Conductivity Meter for Liquids**

Sebastian Plamauer

Matrikelnummer: 3609702

5<sup>th</sup> August, 2016

Betreuer: M.Sc. Timm Severin

Prof. Dr.-Ing. Dirk Weuster-Botz



# **Selbstständigkeitserklärung**

Hiermit erkläre ich, dass ich die vorliegende Arbeit selbstständig verfasst und keine anderen als die angegebenen Hilfsmittel verwendet habe.

---

Ort, Datum

---

Unterschrift

## **Abstract**

# Contents

<b>1. Introduction</b>	<b>7</b>
<b>2. Objectives</b>	<b>9</b>
2.1. Spacial and Time Resolution . . . . .	9
2.2. Electrical Conductivity Resolution . . . . .	12
2.3. Cost . . . . .	12
2.4. Usability . . . . .	12
2.5. Requirements . . . . .	13
<b>3. Background</b>	<b>14</b>
3.1. Theoretical Background . . . . .	14
3.2. Market Research . . . . .	17
<b>4. Design</b>	<b>19</b>
4.1. System Design . . . . .	19
4.2. Electrodes . . . . .	21
4.3. Matrix Switches . . . . .	24
4.4. MinieC Interface . . . . .	25
4.5. Microcontroller . . . . .	28
4.6. Carrier Board . . . . .	29
4.7. Embedded Software . . . . .	30
4.8. OpenSalinity GUI . . . . .	33
4.9. Data Conditioning . . . . .	34
4.10. Bill of Materials . . . . .	35
4.11. Collection of Software . . . . .	36

<b>5. Results</b>	<b>37</b>
5.1. Verification . . . . .	37
5.1.1. Spacial Resolution . . . . .	37
5.1.2. Electrical Conductivity Resolution and Range . . . . .	40
5.1.3. Cost . . . . .	40
5.1.4. Deployability in the Bioreactor . . . . .	40
5.1.5. Usability . . . . .	42
5.2. Validation . . . . .	42
<b>6. Conclusion</b>	<b>46</b>
<b>A. Abbreviations</b>	<b>48</b>
<b>Appendix</b>	<b>48</b>
<b>B. List of Figures</b>	<b>49</b>
<b>C. List of Tables</b>	<b>50</b>
<b>D. Bibliography</b>	<b>51</b>

# 1. Introduction

Fossil fuels play a large role in the worlds energy production and as energy source for transportation vehicles. Especially for vehicles, their high energy density and liquid form at room temperature enabled the construction and operation of cars and airplanes otherwise not possible. At the same time, there are fundamental problems in using fossil fuels as energy source. Be it oil, coal or gas, the formation of these resources is a natural process spanning millions of years. This means that once the current reserves are depleted, they will not be refilled. And even without depleting all the reserves, the depletion of the easily reachable reserves means that ever greater effort has to be taken to find and use less accessible fields, using methods with severe impact on the environment. In addition to that, burning fossil fuels for energy also releases a slew of gases in the atmosphere, of which CO<sub>2</sub> is the most prominent. CO<sub>2</sub> is a greenhouse gas and as such influences the worlds climate tremendously.

In light of those problems, renewable energy sources are needed. For electricity production there are some attractive technologies already in use that directly or indirectly generate power using the sun. For vehicles, using electrical power can be problematic. The electricity has to be stored in batteries, and even with the higher efficiency of electrical motors, the lowered energy density reduces range drastically. Batteries also have to be charged, as opposed to be refilled like tanks, which takes substantially more time. While for some vehicles, like cars, this technology still can be made feasible, it is much less suitable for airplanes.

For these application a more direct replacement for fossil fuels has to be found. A possible solution are bio-fuels. Bio-fuels are generated from biomass, for example plants. An important requirement for the growth of biomass to process to bio-fuel is to avoid competition over land and resources with food production. A low price is also important to make the product economically viable.

One technology to potentially fit these needs are open photobioreactors growing

microalgae. These algae produces lipids, which can be processed to fuel. To improve and optimize these reactors experiments and models are needed. A computational fluid dynamics (CFD) simulation models the flow in the reactor. In order to validate this simulation, experiments measuring the flow conditions in the reactor have to be conducted. To do so, a sensor system needs to be developed. The option explored in this thesis is to measure the streams conductivity. The next chapter details the objectives and criteria of this system.

## 2. Objectives

The goal of this project is the development and test of a low-cost electrical conductivity meter for liquids to be used as an aid to measure and analyze the flow in a photobioreactor.

The method chosen beforehand was to measure the fluids electrical conductivity, which can be changed easily by adding water with differing salt concentrations. Commercially available conductivity meters are built to measure with high accuracy in order to obtain information about a liquids absolute salinity and are relatively expensive. Our use case however does not need to create high accuracy absolute measurements, but measure a relative change allowing to distinguish different liquids by their salinity. However, this needs to happen very fast and at a lot of different points in the stream. The more positions measured, the more complete the picture of the flow becomes. Therefore, the cost per sensor has to be low, to not put a restraint on the total number of points that can be measured.

The actual flow analysis is not part of this work, but rather the creation of a tool to make it possible. As such, the system needs to be designed to be easily usable by people without deep knowledge of the underlying technology.

The following sections describe and detail the requirements the sensor system has to fulfill in order to meet the objectives. These requirements translate the objectives into discrete and verifiable units, serving as the base for development and benchmark for the later performance analysis.

### 2.1. Spacial and Time Resolution

The spacial resolution  $ds$  and the time resolution  $dt$  decide the granularity of the flow image. Both resolutions are connected by the velocity  $v$  of the stream flowing over the

sensor as shown in equation (2.1).

$$v = \frac{ds}{dt} \quad (2.1)$$

With both resolutions connected, only one of them has to be defined.

The information gathered by the sensor has to be granular enough to enable the verification of the simulation. As it is not possible to derive a hard number from that, the following list shows different deliberations to establish a first estimate.

- The granularity of the simulation is determined by the mesh size and is in the order of about 1 mm to 5 mm. A resolution better than that would be unnecessary, making this the lower limit.
- The data collected by the sensor system shows salinity of the liquid passing a certain position over time. By extracting the same data from the simulation, a graph can be compiled comparing the measured to the simulated values. The flow becomes visible when comparing data from different positions. The first sensor to show a spike in salinity is further up the stream than sensors spiking later. The distance between two sensors has to be big enough for a given velocity of the stream so that the time delay can be clearly seen. At a flow speed of  $v$  in the order of 1 m/s, a resolution in the order of centimeters would yield time differences of centiseconds. Whether or not this is sufficient depends on noise and delay in the sensor system, however centiseconds is a conservative estimate likely to be achievable.
- The geometry of the inlet as shown in figure 2.1 also influences the needed resolution. It has to be an order of magnitude smaller as the basins characteristic length, in this case the width of 850 mm, to enable gathering data about the flow conditions within.

Derived from all that, a spacial resolution in the order of centimeters is chosen as requirement.

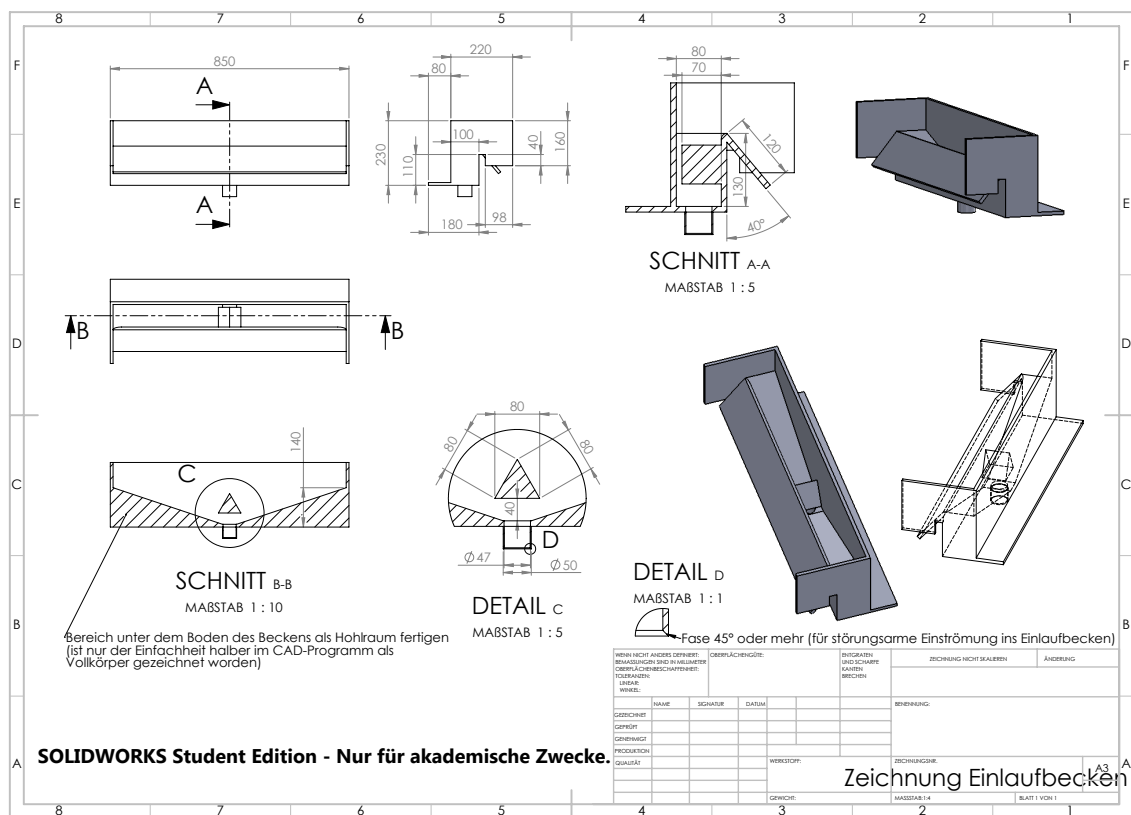


**Figure 2.1.:** The inlet through which the water is fed back from the bottom of the reactor to the top.

## 2.2. Electrical Conductivity Resolution

To measure the arrival of the new water stream after switching the water feed, the system has to be able to distinguish between water with different salinity. The water used normally in the reactor is tap water with a salinity of about 0.2 %. The salinity of the added saltwater can be chosen freely. Water with a salinity of about 5 % is easily available in the facilities and offers a sensible choice. Assuming a reactor with 65 l in circulation and an added saltwater impulse of 5 l, the resulting salinity after perfect homogenization would be approximately 0.5 %. The system has to be able to clearly distinguish between all those salinities. The sensors sensitivity therefore shall be better than a change of 0.1 % salinity with a range from 0 to 5 %.

## 2.3. Cost

The more sensors used, the more points in the stream can be measured and the better the image of the stream gets. Therefore, the cost per sensor has to be low enough to not be prohibitive of adding more sensors. The cost of a high quality lab conductivity meter is in the range of €1000 and was set as the goal of maximum cost for the sensor system. The number of sensors needed to cover all interesting regions of the bioreactors is about 40. A maximum cost per sensor of €25 results from those figures.

## 2.4. Usability

The sensor system is meant to be used in the algae reactors of the algae cultivation center at the Ludwig Bölkow Campus. It has to be possible to easily mount and remove the system to and from the reactor without having to dismantle it.

The system also has to be easy to use, so it can be helpful to the researchers working on the reactor. It has to work reliably and act according to expectations of the users. The chance of handling errors that lead to loss of data has to be minimized. All operations have to be documented in a minimal set of written instructions, so the system can still be used even if the designer is not available anymore.

## 2.5. Requirements

The table 2.1 concludes and displays all requirements alongside the methods of verification to be used.

**Table 2.1.: Requirements**

Nr.	Requirement	Verification
1	The system shall have a spacial resolution in the order of 10 mm.	Test, Inspection
2	The system shall have a sensitivity of 0.1 % salinity.	Test
3	The system shall have a range from 0 to 5 % salinity.	Test
4	The cost per sensor shall be less than €25.	Analysis
5	The system shall be deployable in the algae reactor.	Demonstr.
6	The system shall be usable with a minimal set of written instructions.	Test, Review

# 3. Background

In this chapter a theoretical background of electrical conductivity measurement will be established. After that, a market research takes a look at the commercially available solutions of sensor systems and parts that could be used to develop one.

## 3.1. Theoretical Background

The following section is translated and summarized from the books [7] and [6].

The conductivity  $\kappa$  is the ability of a certain volume of a substance to conduct electricity. It is measured in the unit  $S/m$  and is a specific parameter normalized to the length and cross section of the volume. Conductivity in a liquid depends on ions as charge carrier and can therefore be used to measure its concentration.

To better understand conductivity, an equivalent circuit diagram, shown in figure 3.1, of an electrode system shown in figure 3.2, can be used. This method is called conductometry and in this form a two-electrode-cell is used. In this measurement configuration, two electrodes are submerged in the liquid to be measured and a voltage is applied. The resistance  $R$  of the substance is determined by measuring the potential drop  $U_R$  given a constant voltage  $U$ , current  $I$  and internal resistance  $R_i$ .

The resistance  $R$  is

$$R = \frac{U_R}{I} \quad (3.1)$$

The inverse of the resistance  $R$  is the conductance  $G$

$$G = \frac{I}{U_R} \quad (3.2)$$

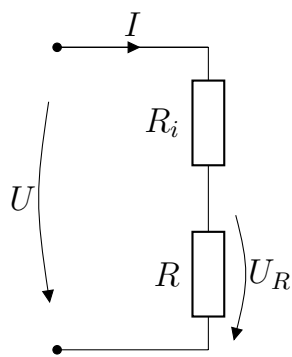


**Figure 3.1.:** equivalent circuit diagram

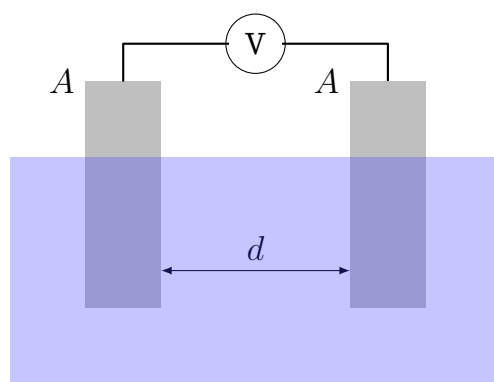


**Figure 3.2.:** electrode configuration

The cell constant  $C$  describes the geometry of the sensor

$$C = \frac{d}{A} \quad (3.3)$$

where  $d$  is the distance between and  $A$  the surface area of the electrodes.

Considering the cell constant  $C$  finally yields the conductivity

$$\kappa = G \cdot C \quad (3.4)$$

In electrolytes, the electrical conduction is a result of mass transfer, where ions are carrying the charges. If the measurement is conducted with direct current, this mass transfer leads to changes in the measured solution and the electrode surface, negatively impacting the measurement. Furthermore, polarization effects create additional resistance, leading to lower than actual results. To avoid this, alternating current is used. The fast, periodical swap of polarity eliminates the net mass flow and its effects. Polarization is a result of the current flowing through the electrode, thereby its effects can be minimized by minimizing this current. One method to do this is replacing the two-electrode-cell with a four-electrode-cell. This separates the current flow from the potential measurement by using one electrode pair to apply the current, and a separate pair to measure the potential drop.

The electrolyte's temperature affects the mobility of the ions and thereby also has a big influence on the conductivity. It has to be taken in account when comparing two measurements. If the temperature  $T$  is known, the conductivity at that temperature  $\kappa_T$  can be normalized to a reference temperature  $T_{ref}$  using equation (3.5), resulting in the reference conductivity  $\kappa_{ref}$ .

$$\kappa_{ref} = \kappa_T \frac{1}{1 + C_T \cdot (T - T_{ref})} \quad (3.5)$$

The temperature coefficient  $C_T$  assumes a linear correlation and is only valid in a narrow temperature range. For bigger ranges the denominator can be replaced with

a polynomial using higher order coefficients, resulting in equation (3.6).

$$\kappa_{ref} = \kappa_T \frac{1}{\sum_{i=0}^n C_{Ti} \cdot (T - T_{ref})^i} \quad (3.6)$$

## 3.2. Market Research

Conductivity meters can be readily bought and range from prices of over €1000 for lab equipment [4] to €100 for simple field water quality monitors [5]. Even cheaper water quality testers from no-name manufacturers can be found for as little as €10 from online vendors.

Figure 3.3 shows a field conductivity meter from a quality manufacturer as example for the typical traits most available solutions share:

- a single electrode pair
- a display to report measurements
- designed to perform singular reads with high quality

While field conductivity meters have the electrodes integrated to form one compact device, the more expensive lab equipment often has the electrodes attached to the device with a cable, allowing for a more flexible use.

A different option was found in the MinieC I2C eC interface from Sparky's Widgets [3]. The MinieC interface is an Open Hardware project providing a conductivity sensor that easily interfaces with a microcontroller, licensed under Creative Commons [1]. This license allows to study the original design files and build modified versions. Ready-made boards can be purchased for about €25.

The design approach of this solution is also more modular than that of the more professional equipment. The MinieC offers an interface to connect external electrodes and can be controlled and read by a microcontroller.



**Figure 3.3.:** Fisher Scientific™ Traceable™ Salinity Meter Pen [5]

# 4. Design

This chapter describes the design of the sensor system and all components involved. It system consists of several parts playing different roles. The Chapter 4.1 System Design gives an overview of these parts, their purpose and their communication with each other. Afterwards, these subsystem are described in detail.

## 4.1. System Design

The system as shown in Figure 4.1 is designed as follows:

On the user-facing side there is a personal computer (PC). This PC runs software that visualizes a live data stream and provides a control interface for the sensor system. It is connected via USB to a microcontroller. This microcontroller controls the MinieC interface via the Inter-Integrated Circuit (I2C) communication protocol, reads the measurement data from it and sends it to the PC. It also controls the matrix switches via the Serial Peripheral Interface Bus (SPI). The MinieC Interface provides the signal (SIG) and ground (GND) between which the resistance is measured. Both lines are connected to one matrix switch each. These matrix switches are able to connect one input to 8 different outputs. On each of those outputs, one electrode is connected. The matrix switches can thereby connect the MinieC interface to one of 8 electrode pairs at a time.

To add further sensors to the system, two strategies are possible:

- by chaining up multiple stages of matrix switches, the number of electrodes can be increased eightfold with each stage
- by connecting another MinieC Interface with its own set of matrix switches to

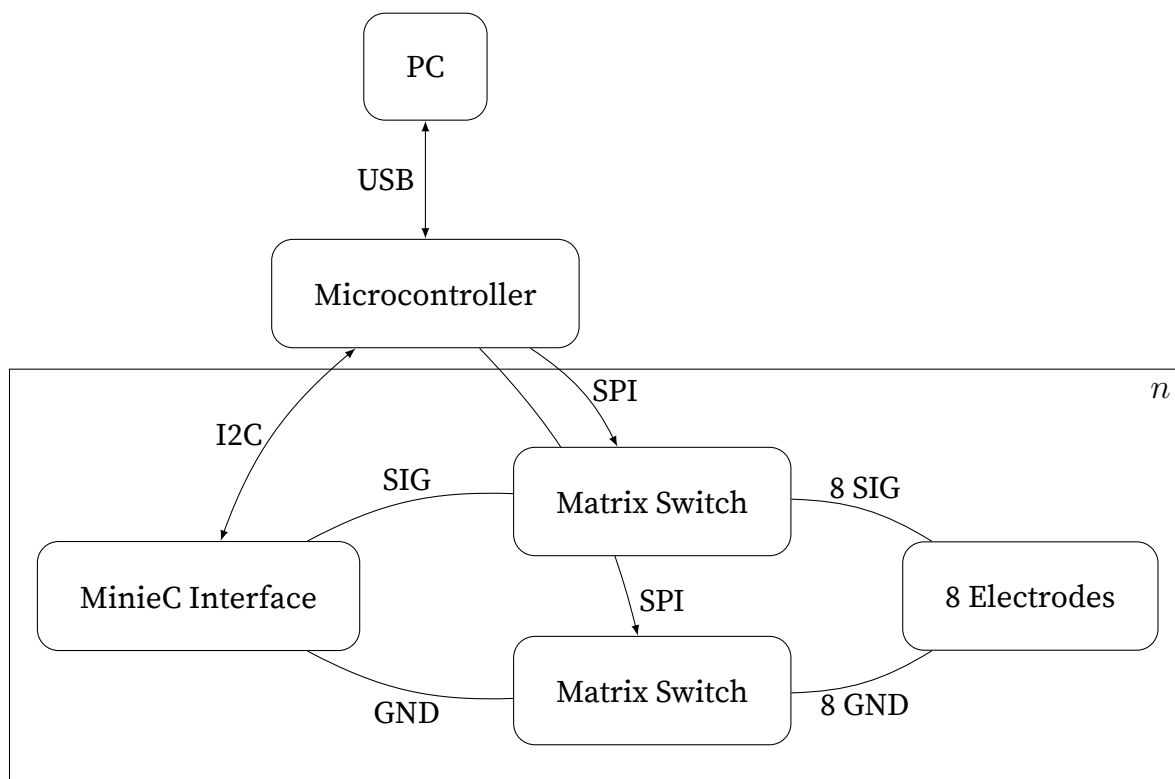


**Figure 4.1.:** System Design

the microcontroller, 8 more electrodes can be added with each of these subsystems

The first option results in lower cost per added electrode, as the MinieC interface is reused. However, with a system like that, all electrodes have to be read in serial, while with the second option each MinieC interface can be read in parallel, resulting in a higher sample rate. Practically the second option is also easier to achieve. For the first option, a board with 18 matrix switches and 80 connections is needed, while the second option only uses 2 switches per board resulting in 16 connections. The simpler board greatly reduces complexity and can also be made smaller.

## 4.2. Electrodes

The electrode pairs are the actual sensors in contact with the fluid to be measured. Their material and geometry influence the measuring range of the system. According to information in the book [7] a cell constant  $C$  of 1 enables a range from  $2 \cdot 10^3 \mu\text{S}/\text{cm}$  to  $10 \cdot 10^3 \mu\text{S}/\text{cm}$ . For a water temperature of  $18^\circ\text{C}$  this corresponds to salinities of 0.66 % and 0.12 %. While this theoretical range is not sufficient for our purpose, first tests showed that the achievable range is much bigger than described in the book. The book doesn't specify the materials influence on the range and it also doesn't qualify how the usable range is defined. As our application has much lower demands on accuracy as the usual ones, this might be an explanation for the discrepancy.

Figure 4.2 shows the geometry of the sensor. To achieve a cell constant  $C$  of 1, a width  $w$  of 1 mm, height  $h$  of 10 mm and distance  $d$  of 10 mm were chosen.



**Figure 4.3.:** A handmade sensor strip.

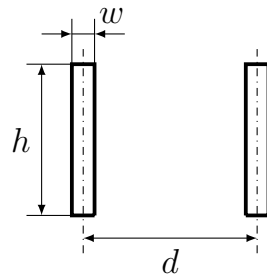


**Figure 4.2.:** An electrode pair forming a sensor.

As a first proof-of-concept a sensor array was built, containing multiple electrode pairs on a strip, pictured in figure 4.3. A 50 mm wide and 250 mm long band of Kapton adhesive tape served as the base. 4 electrode pairs made from 0.2 mm platinum wire were arranged equidistant on the strip. 0.4 mm enameled copper wire runs along the tape to connect each electrode pair to the left end of the strip, from which insulated cables run to the sensor node. After soldering the joints, two smaller strips of tape were used to cover the wiring, exposing only the electrodes to fluid.

First tests with this sensor array showed the viability of the concept, however a simple look at it shows the inherit problems. Instead of a uniformly flat strip with minimal influence on the flow, the assembly forms several irregularities. Soldering 0.2 mm platinum wire to 0.4 mm enameled copper wire on a piece of adhesive tape per hand also did not result in clean solder joints. And while with the experience of the first array, the second array turned out a bit cleaner, the fundamental problem remains: it is a tedious manufacturing process resulting in a low quality product.

As an alternative to these handmade strips, industrially produced Flex-PCBs were



**Figure 4.4.:** The sensor strip design to be implemented as flexible PCB.



**Figure 4.5.:** A sensor strip manufactured by LEITON and assembled with cables and waterproofing.

identified. Flex-PCBs are flexible printed circuit boards that are very close to the hand-made arrays described above. They also use Kapton as base, on which a copper coating gets applied and is partially removed by etching to form the conducting paths. On top, another layer of Kapton is applied, with cutouts in the places where the copper is supposed to be exposed. The exposed copper is then plated with ENIG (Electroless nickel immersion gold) to protect the copper from oxidation and provide the landing pads for electrical components to be soldered on.

For our purpose those exposed and plated landing pads can be used as electrodes, being nicely embedded in a FlexPCB that also runs the wiring up to an interface from where cables can be run. Using the FlexPCB itself as cable is not viable due to the high cost per area. Instead, cables are soldered directly to the PCB and silicone is used to create a waterproof seal around the connection.

The final design for the sensor strip, as shown in figure 4.4, implemented as a flexible PCB consisted of 4 electrode pairs spaced 50 mm apart. The strip is 25 mm wide and 220 mm long. 16 pieces were manufactured by LEITON for a price of €376.47, resulting in a price per strip of €23.53 and of €2.94 per sensor. Figure 4.5 shows a sensor strip with attached cables and silicone waterproofing.

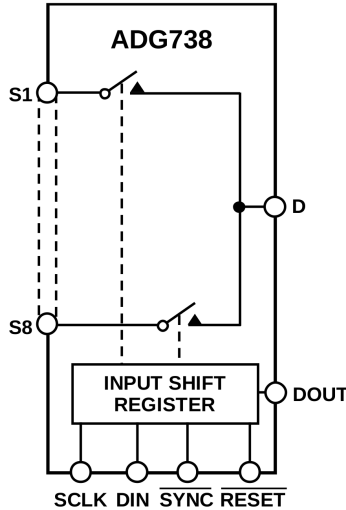


**Figure 4.6.:** Functional block diagram of ADG738

### 4.3. Matrix Switches

The matrix switches are an essential part of the system, enabling it to use multiple sensors with a single MinieC Interface, thus lowering the cost per sensor. The part used is an ADG738 from Analog Devices. It is an 8-channel CMOS analog matrix switch controlled via a 3-wire serial interface. The following information is taken from the data sheet [2].

Figure 4.6 shows the functional block diagram. The switch has one drain pin (D) and 8 source pins (S1..S8). Despite the naming of drain and source, the internals provide simple switches between the drain and each source pin. The switches work in both directions without any restriction on the signal beyond a maximum current of 120 mA that far exceeds our needs. By sending control commands via the 3-wire interface, each of the 8 internal switches can be turned on and off individually.

The example timing diagram 4.7 describes the data transmission process. The microcontroller sends one byte of data to the matrix switch. Each of the 8 bits of this byte controls one switch. The first bit controls the first switch and so on. If the bit is 1, the switch is closed, if 0, the switch is open. To send the byte, first the synchronization pin (SYNC) has to be pulled low from its usual high level. A clock signal is provided

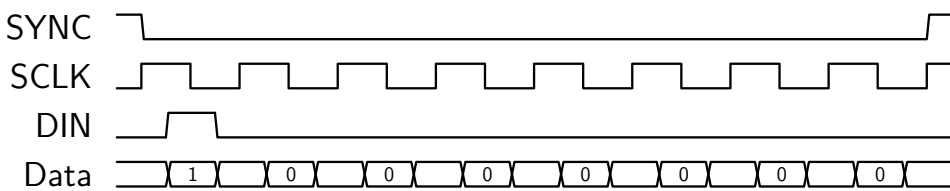


**Figure 4.7.:** Timing diagram

to the clock pin (SCLK). At each falling edge of the clock signal, the data input (DIN) is read - where high leads to a 1-bit and low to a zero-bit. After 8 cycles, SYNC is pulled high again marking the end of data transmission with a full byte transferred. After that, the switches immediately take their instructed states with switching times in the order of 100 ns. In the example shown, the first switch is on, while all others are off.

Multiple matrix switches can be controlled at once by daisy-chaining the data output pin (DOUT) of the first device to DIN of the second one, and on so forth. Both SYNC and SCLK are connected to the same bus. This assures that all matrix switches are set in the same state and at the same time.

Prices for the ADG738 start at €3.89 for a single chip but drop below €3 when the order exceeds 50 pieces. The parts used in the prototypes were free samples provided by the manufacturer Analog Devices.

## 4.4. MinieC Interface

The MinieC Interface contains the electronics to perform the resistance measurement. It contains several parts used to generate an electrical signal, run it through a circuit in which the liquid to be measured serves as a resistor and measure the voltage drop over it.

The first part is a TPS6040 charge pump voltage inverter. Its purpose is to generate a negative output voltage from a positive input. This negative voltage and the positive voltage are needed to drive a Wien bridge oscillator. This oscillator outputs a sine wave voltage oscillating between the positive and negative input voltage. This whole

first stages purpose is to generate an alternating current to be used in the measurement, avoiding the polarization effects described in the background chapter.

The AC signal provided by the first stage is then fed into an OpAmp. An OpAmp is a part that has two input signals and one output, where the output is proportional to the difference of the input signals. In our use case, the OpAmp's output is pulled to ground via a voltage divider. The first resistor  $R_i$  in the divider is fixed, while the second one  $R$  is the liquid to be measured. The output voltage of this divider is depended on the liquids resistance. This voltage is then fed back into the second input of the OpAmp. Via this feedback, the output (OUT) of the OpAmp is now the input signal (SIG) modulated in amplitude by the resistance of the liquid.

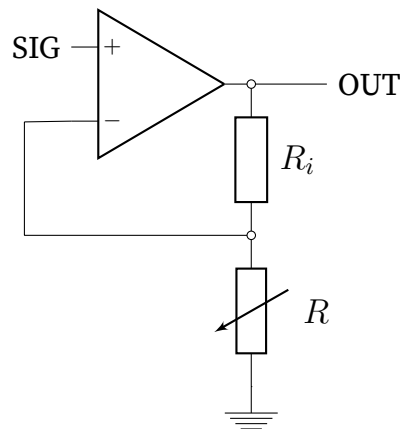


**Figure 4.8.: OpAmp**

In the last step, the modulated output is amplified in two stages, filtered, and then measured by an analog-digital-converter (ADC). The ADC measures the voltage and provides the measurement to the microcontroller via I2C.

First test of the interface surfaced an interesting problem. The graph displayed in figure 4.9 shows the response to an immediate switch from the AC input signal to zero. The first red line marks the moment of the switch, the second line marks the moment when the response reached the voltage zero. The red dot marks the moment when the response reached the midpoint between the old and new input. It took 40 ms for the response to follow the input. This slow response time is not acceptable in our system

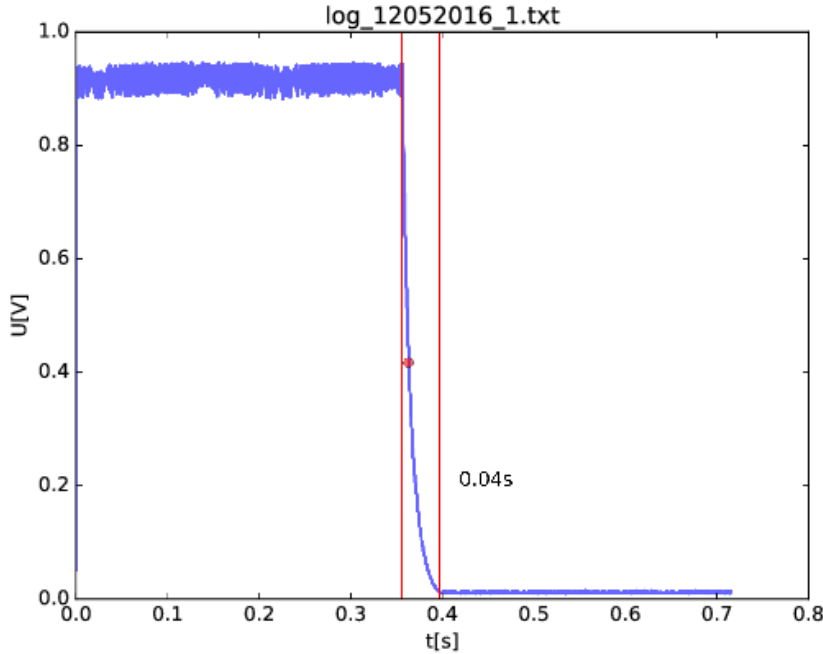


**Figure 4.9.:** After the switch, the capacitor discharges slowly.

because it prohibits the switching between sensors. The slow response would smear the measurement over all sensors and it would not be possible to measure a difference between them. Waiting for that amount of time between each read of a sensor would reduce the time resolution to a level where the desired information can no longer be extracted from the data. The cause of this behavior is the filter placed before the ADC. As the output of the OpAmp is an alternating current, a diode and a filter capacitor are used to generate a direct current signal proportional to the amplitude of the AC signal. This is done so the sample rate of the ADC does not have to match the frequency of the signal, which makes it easier to use when fast sampling rates are not necessary.

Figure 4.10 shows the response to the same switching as before, but with the filter capacitor removed. The diode is still in place and removes the negative voltages from the output. Without the capacitor however, the signal oscillates with the same 1666 Hz as the Wien bridge oscillator provides. Because the sample rate of the ADC is not as fast as the oscillation, it measures at random moments on the sine wave, resulting in an output that moves between zero and the maximum amplitude. The red line again

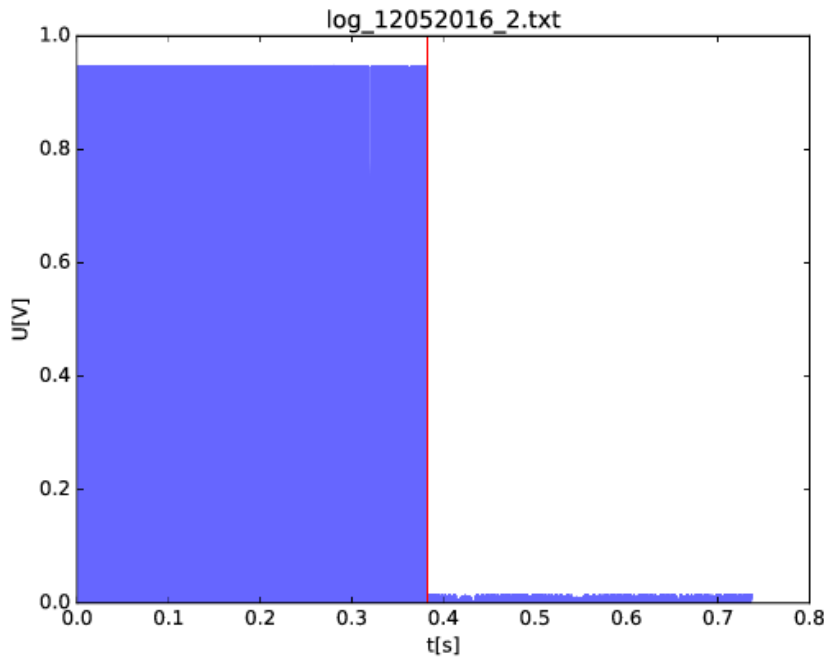


**Figure 4.10.:** The response immediately follows the switching event, but the AC signal is now unfiltered.

marks the moment of the switch and it can be clearly seen that the response delay is now gone. The oscillating behavior that was electrically filtered before, now can be filtered digitally without the sensors influencing each other.

The MinieC-Interface costs about €22 depending on exchange rates.

## 4.5. Microcontroller

The microcontroller has to be able to control the functions of the sensor nodes attached to it, read the data from them, log it and serve it to the user-interface. They usually are programmed in C or C++, however in recent years other options emerged. One of those is Micropython, which is an implementation of the Python 3 programming language designed to run on microcontrollers. Python is a vastly easier language to work with than C/C++, and this is especially true when the involved persons are not from a computer science or electrical engineering background, but i.e. mechanical engineering or other sciences. In those fields, Python is often familiar from usage for

data processing and visualization. Using Micropython enables us to design a system where it is more likely that the people using it are able to understand the code, enabling them to improve it and adapt it to alternate use-cases. It does however limit our choice of hardware to supported platforms and it requires more powerful and thereby expensive micro-controllers. But as the system only requires one microcontroller to drive a very large amount of sensors, the added cost is relative and outweighed by the benefits of the better usability.

For prototyping, a development board named "Espruino Pico" was chosen. It is a very small and simple board that provides the electrical boilerplate to use a micro-controller without needing to deal with the lowest level of electronics, like cleaning power supply, USB connection and so on. The board costs €35.

## 4.6. Carrier Board

The carrier board is a simple PCB implementing all parts described above. Figure 4.11 shows the assembled board. On the left, the Espruino Pico board can either be soldered directly to the PCB or plugged in using pin header connectors. Above and beyond used pins are replicated on through-holes. This allows for easy connection of measurement equipment to debug the system during development, but can also be used later to connect carrier boards together. Only one would carry a microcontroller and control the other connected boards.

In the middle there are two matrix switches. They can either be directly soldered on as in this image or they can be soldered to an adapter board that is again mounted to the carrier with pin header connectors in the inner rows of through-holes. The outer through-holes are where the connectors for the cables to the sensors are mounted.

On the right side the MineeC Interface is mounted. It also can be either directly soldered or use pin header connectors.

The design is tailored to the use as a prototype. That means that everything is made a bit bigger than necessary, which allows for easier modifications. It also is kept modular, so that each part can be swapped out easily. A later redesign would integrate all

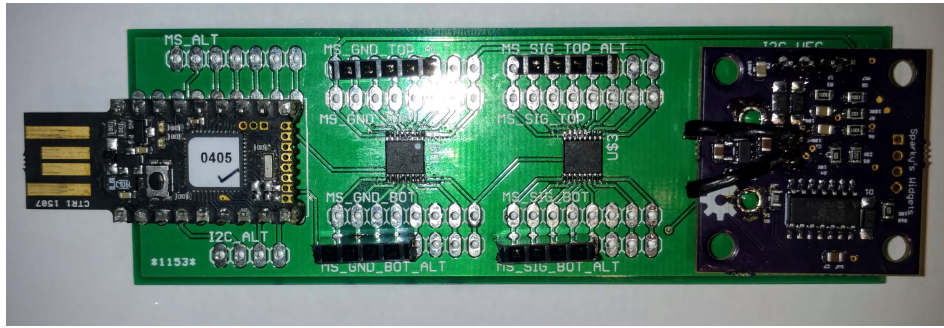


**Figure 4.11.:** The assembled carrier board with all parts mounted.

boards into one and try to reduce size, which in turn saves money on PCB manufacturing. However, the prototype showed no design errors and is fully functional, so the next design step is only necessary when more boards are needed.

The carrier boards were manufactured by [dirtyPCBs](#), a very cheap service for prototype boards. The total cost for 10 pieces was around €50, depending on conversion rates, of which about €30 were shipping costs from China to Germany. The low price comes with low quality, as the name of the service already suggests, but for prototypes the trade-off is well worth it.

## 4.7. Embedded Software

The embedded software is the program running on the microcontroller. As already described in section 4.5, [Micropython](#) is used to implement this program.

As soon as the system is powered up, it starts listening for the Start and Stop commands from the OpenSalinity GUI running on the host PC. Once it receives the Start command, it starts polling the sensors and delivers the data to the PC, where it is captured. In order to poll the sensors, the program has to control the switches and the ADC. It first switches both matrix switches to a certain electrode pair and then reads the ADC value for it. After that it switches to the next pair and thus circles through all connected sensors. Each ADC read is accompanied by a time stamp for the read.

The data is sent in a simple format described in the listing 4.12. One line contains

timestamps and values for all  $n$  connected sensors separated by one whitespace. The line ends with the newline character.

```
1 <time 1> <value 1> <time 2> <value 2> ... <time n> <value n> \n
```

**Figure 4.12.:** Data Format

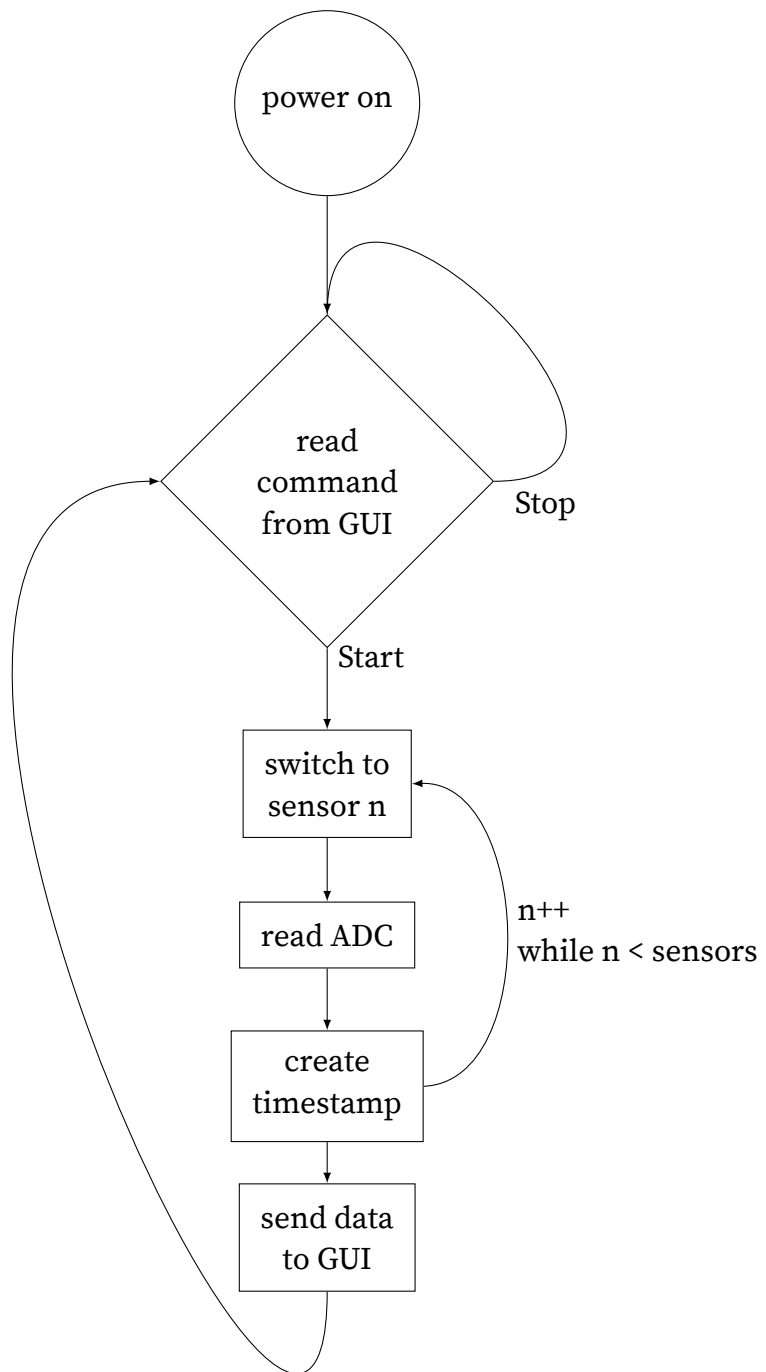


**Figure 4.13.:** Embedded Software Flow Diagram

## 4.8. OpenSalinity GUI

The OpenSalinity GUI is a program designed to simplify and aid the usage of the sensor system. It provides following functionality:

- Storing all sensor data to a file.
- Choosing a file to which the data is stored.
- Starting and Stopping the data capture.
- Visualize the data.

The data capturing can not be started before a file to save to is chosen, to avoid the unintentional loss of data. The Save button allows to create the file to be written to and offers a default file name containing the date and time of the creation, helping to keep the data logs in order. The live visualization is a bar graph showing each sensors current measurement, allowing to monitor the ongoing experiment. In addition to size, the bars are also color coded, shifting from red to blue with increasing salinity.

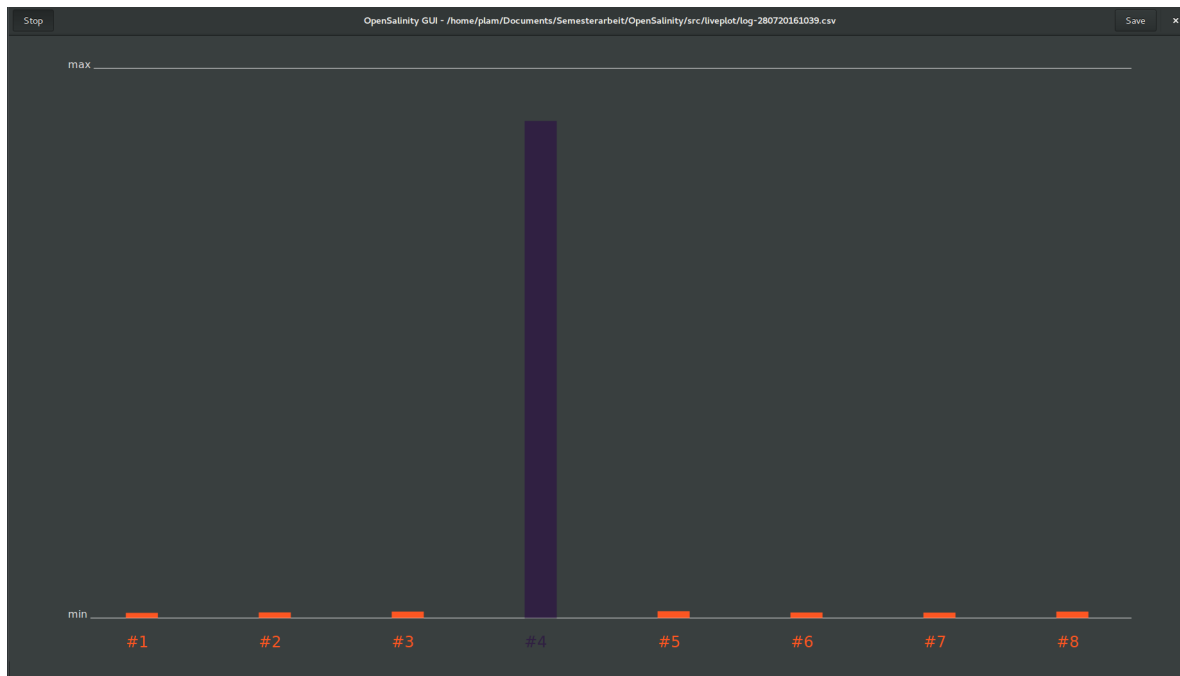


**Figure 4.14.:** OpenSalinity GUI

The software again is written in Python, using GTK+ as GUI toolkit and pyserial to communicate with the microcontroller. It was developed and tested on a Linux based operating system, however due the nature of the used programming language and toolkits it is cross-platform and can be run on Windows and OSX also.

In addition to or as replacement of the GUI, a set of command line tools can be used. These tools allow for a redundant capturing of the sensor data and for an alternate visualization. A detailed manual on how to use those tools as well as the GUI is provided in the Appendix.

## 4.9. Data Conditioning

Before the data can be analyzed it has to be conditioned to deal with certain peculiarities of the embedded software. This is done in post processing rather than during the data capturing to minimize overhead and retain high sampling rates.

The microcontroller measures time since start up by counting clock cycles. These are converted to microseconds stored as an integer value. The microcontroller is a 32-bit architecture, however the Micropython implementation uses 2 bits for data type identification, leaving 30 bits for data. This means the counter can count from  $-2147483647$  to  $2147483647$ , meaning that it wraps around roughly every 8.9 minutes. In the data conditioning phase, these wrapping times are translated to a rolling time since start-up. This is done by scanning for the first time value that is smaller than its predecessor and then adding the value of  $2^{30}$  to all following values. This is repeated until all time values are corrected. Figure 4.15 visualizes the algorithm.

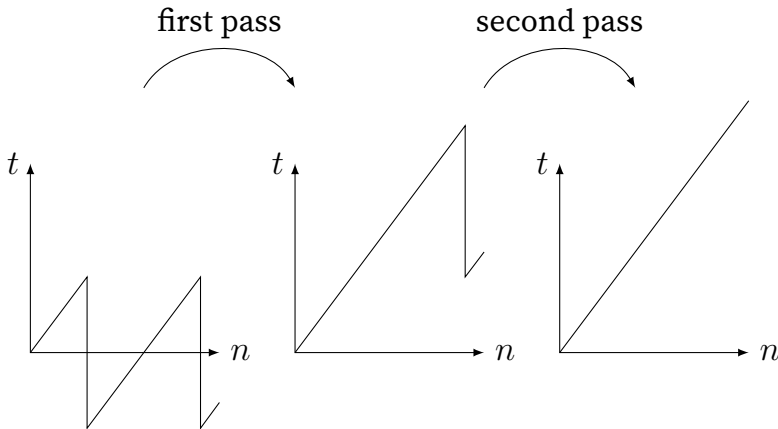


**Figure 4.15.:** Fixing the integer wrap of the time variable.

## 4.10. Bill of Materials

The bill of materials collects all used components, their price and a possible source in the Table 4.1. Except for the MinieC Interface multiple sources are available for all parts. In case it becomes unavailable, the hardware design files are provided to have them manufactured by a different source. The Espruino Pico also comes from a small manufacturer and may not be available in the future. However, alternatives are plentiful and can be used either with simple jumper cables or by redesigning the carrier board.

The carrier board and sensor strip are made to order by PCB makers. Generally, any manufacturer will be able to produce the boards with the provided design files, however the size limits and corresponding prices can vary. The prices also strongly depend on lot size. The prices in the table are the prices per piece for a lot of ten carrier boards and 16 sensor strips.

**Table 4.1.: Bill of Materials**

Nr.	Qt.	Name	Source	Price
1	1	Espruino Pico	watterott.com	€26.95
2	1	Sparky's Widgets MinieeC Interface	sparkyswidgets.com	€21.66
3	2	Analog Devices ADG738	mouser.de	€3.89
4	1	Carrier Board	dirtypcbs.com	€4.87
5	2	Sensor Strip	leiton.de	€23.53
6	1	USB Extension Cable	amazon.de	€5.49
7	1	Flat Ribbon Cable 40-pole	amazon.de	€7.99

## 4.11. Collection of Software

# 5. Results

In this chapter the verification and validation of the developed sensor system are described. The verification is a set of tests designed to review whether or not the system meets the requirements specified in the Chapter 2 Objectives. The validation is done by analyzing the data gathered during a number of experiments in the bioreactor.

## 5.1. Verification

### 5.1.1. Spacial Resolution

Requirement: The system shall have a spacial resolution in the order of 10 mm.

An inspection of the physical size of the sensor and their placement on the array, drawn in Figure 5.1, shows us a sensor size of 10x11 mm arranged on a grid of 25x50 mm. The theoretical minimal grid size achievable with the chosen sensor size and a minimum distance between electrodes of 1 mm is 11x12 mm. This grid size is the physical limitation of the spacial resolution and by being well within the order of 10 mm meets the requirement.

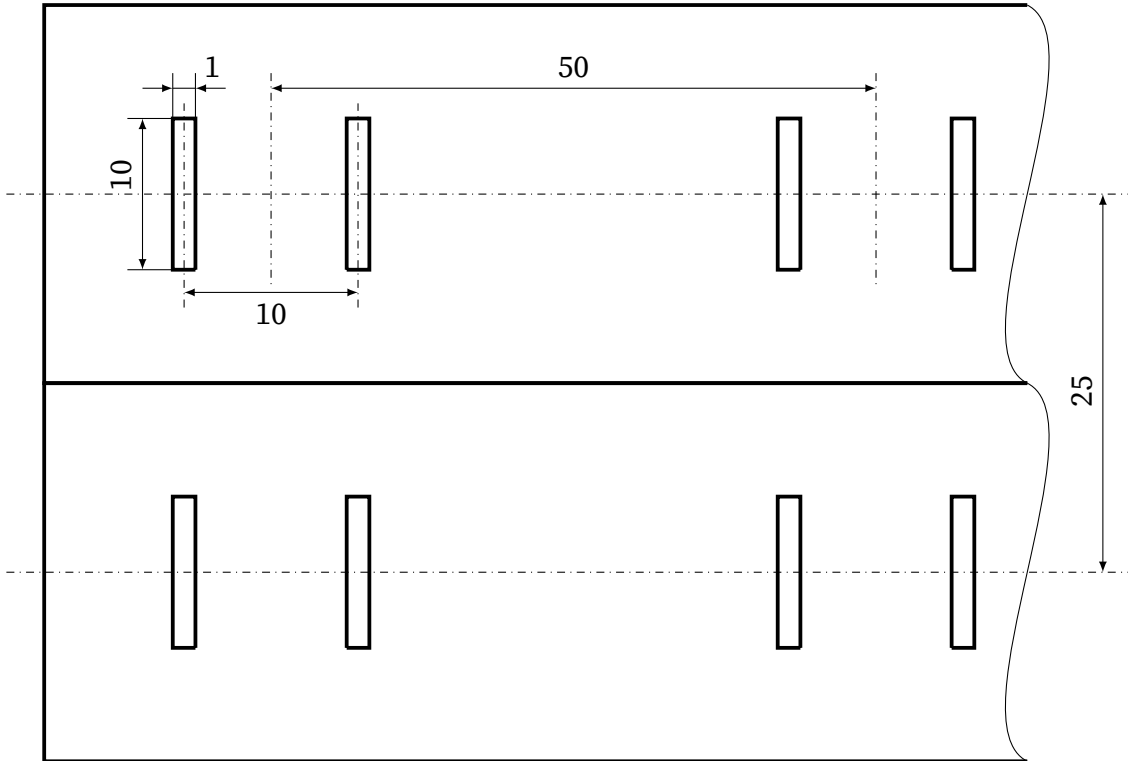


**Figure 5.1.:** A dimensioned drawing of the sensor grid made up by two strips placed next to each other, not drawn to scale and cut on the right side. It shows the sensor size of 10x11 mm, the horizontal distance between sensors of 50 mm and the vertical distance of 25 mm.

Due to the coupling of the spacial and time resolutions via the streams velocity as shown in Equation (5.1), this however is not sufficient to verify the requirement.

$$v = \frac{ds}{dt} \quad (5.1)$$

A spacial resolution of 10 mm would require a time resolution of 0.01 s. However, this assumes the size  $l$  of the sensor and the time  $\tau$  a measurement takes to be infinitesimal small, which in reality it is not. While the sensors measures, the flow continuous and instead of measuring the conductivity of a certain volume at a certain time, an average is measured. Figure 5.2 visualizes this issue.

To accommodate for that, factors  $n$  (5.2) and  $k$  (5.3) are introduced, describing the ratio of the resolutions to the actual sizes.

$$n = \frac{l}{ds} \quad (5.2)$$

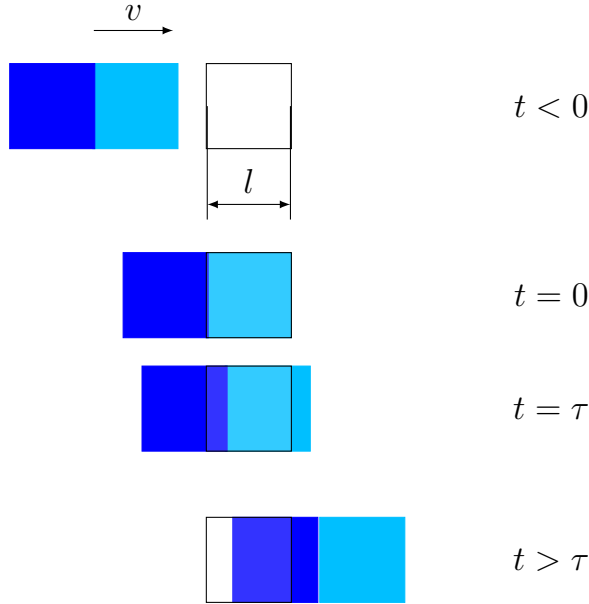


**Figure 5.2.:** The control volumes in blue have the same size as the sensor (black rectangle). At  $t = 0$  the measurement starts and the first control volume is directly over the sensor. When the measurement ends at  $t = \tau$  the control volumes have moved. The sensor is covered by a mix of the two volumes.

$$k = \frac{\tau}{dt} \quad (5.3)$$

Inserting  $k$  and  $n$  in Equation (2.1) yields:

$$v = \frac{ds}{dt} = \frac{k \cdot l}{n \cdot \tau} \quad (5.4)$$

The ratio  $r$

$$r = \frac{k}{n} \quad (5.5)$$

is the ratio of the time it takes a control volume to enter and leave the sensor area to the time a measurement takes. Its inverse is the movement of the control volume during the measurement time and thereby the percentage by which the measured volume is bigger than the control volume. A ratio of 1 on would mean the measured volume is two times the sensor size, thereby halving the spacial resolution. To keep the resolution close the the sensor size, a ratio of 4, increasing the measured volume by 25 % is viable. With the given sensor size and flow speed, a measurement time  $\tau$  of 0.0025 s

or 2.5 ms is needed.

To test if the time resolution matches this, the measurement time itself can be timed. The difference between two adjacent times, i.e. the first time (975209221 ns) and the second time (975209961 ns), in the data set in Listing 5.1 is the measurement time of 740 ns. The mean of the differences through the whole data set is 748 ns. This means that the measurement is more than three times faster than required, showing that the time resolution easily matches the spacial resolution.

**Listing 5.1:** An excerpt of measurement data showing three lines of data from eight sensors. The long numbers are the times at which the measurements were taken in nanoseconds measured from the start, the short numbers are the measured values.

```
1 975209221 21 975209961 59 975210676 15 975211397 0 975212119 0 975212840 26  
    975213554 59 975214276 9  
2 975215877 57 975216602 42 975217324 0 975218046 0 975218761 0 975219482 61  
    975220204 43 975220919 0  
3 975222520 52 975223271 0 975223993 0 975224708 0 975225429 45 975226150 53  
    975226867 0 975227583 0
```

### 5.1.2. Electrical Conductivity Resolution and Range

Requirement: The system shall have a sensitivity of 0.1 % salinity.

Requirement: The system shall have a range from 0 to 5 % salinity.

### 5.1.3. Cost

Requirement: The cost per sensor shall be less than €25

### 5.1.4. Deployability in the Bioreactor

Requirement: The system shall be deployable in the algae reactor.

The deployability was demonstrated during two test campaigns on the reactor. Figures 5.3 and 5.4 show the set up during the tests. The host PC can be placed on a desk

beside the reactor and connected to the carrier board with a USB cable. The carrier board can also be placed on desk or temporarily mounted on the reactor. The sensor strips connect to the carrier board with 1 m long cables and are attached to the reactor with electrical tape.



**Figure 5.3.:** The sensor strips are mounted to the bioreactor with electrical tape. Cables of 1 m length run towards the carrier board which is not in the frame.

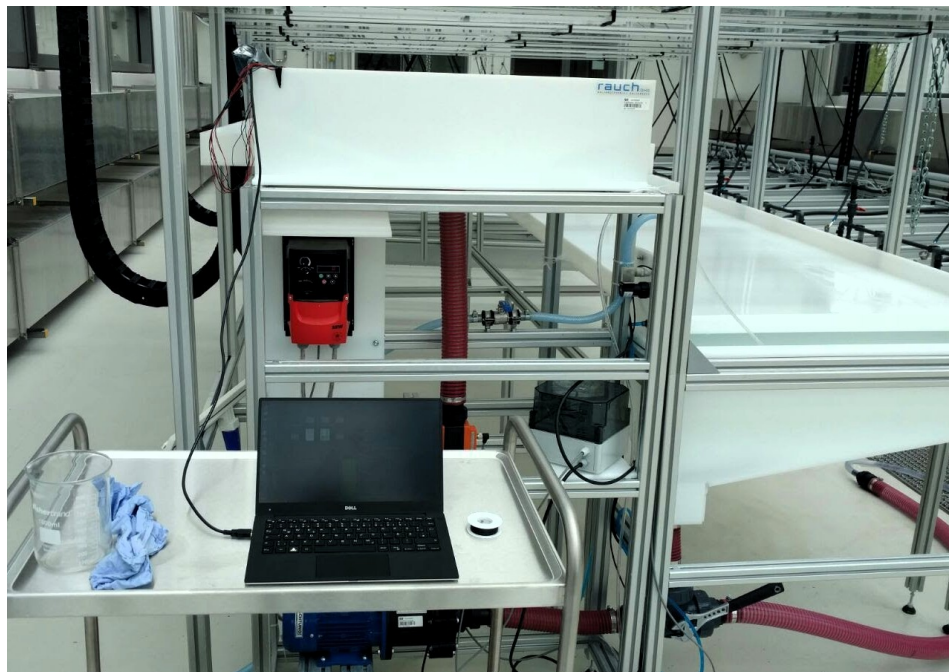


**Figure 5.4.:** A laptop is used as host PC. A USB cable connects to the microcontroller on the carrier board, which is mounted on the side of the inlet basin.

### 5.1.5. Usability

Requirement: The system shall be usable with a minimal set of written instructions.

## 5.2. Validation

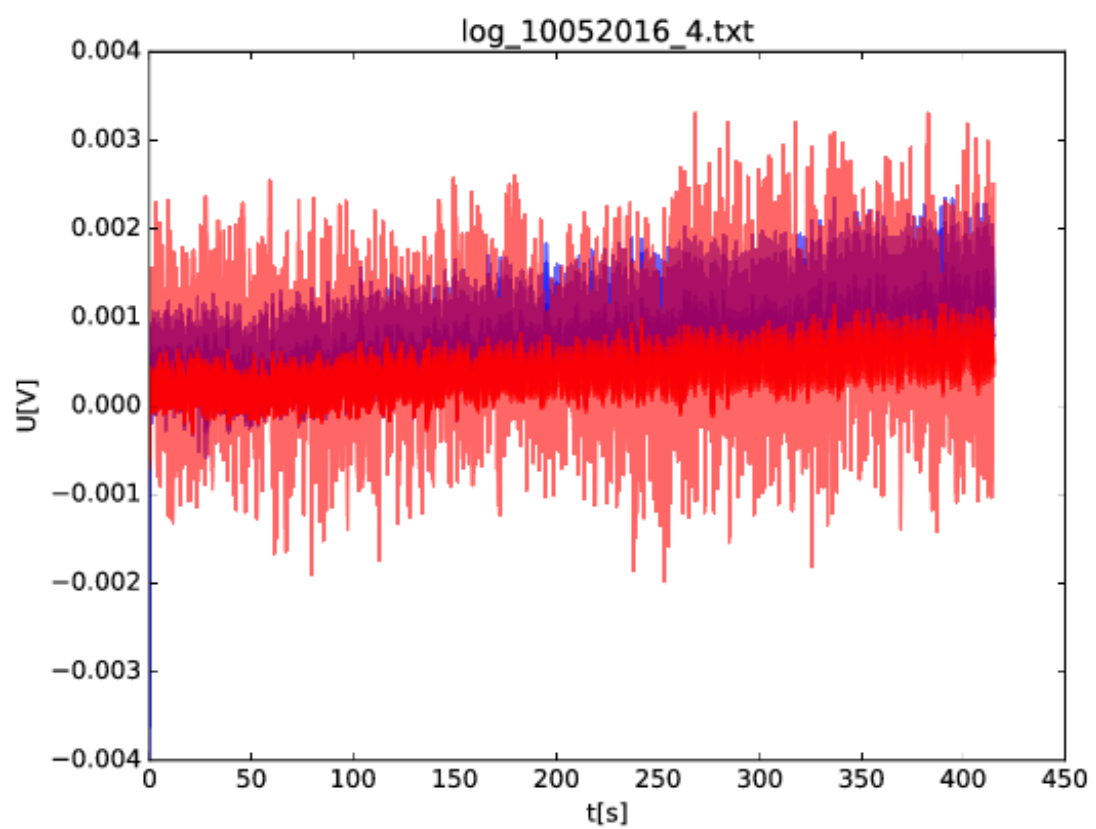


**Figure 5.5.:** noise

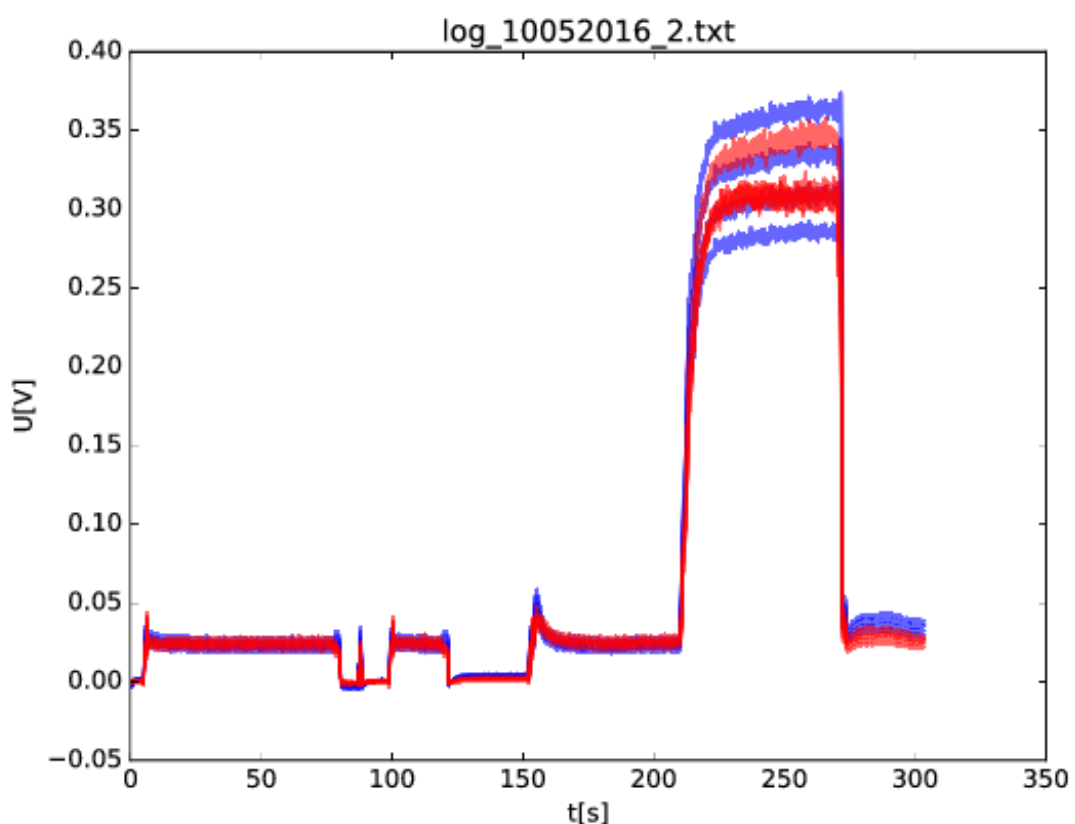


**Figure 5.6.:** feed switch

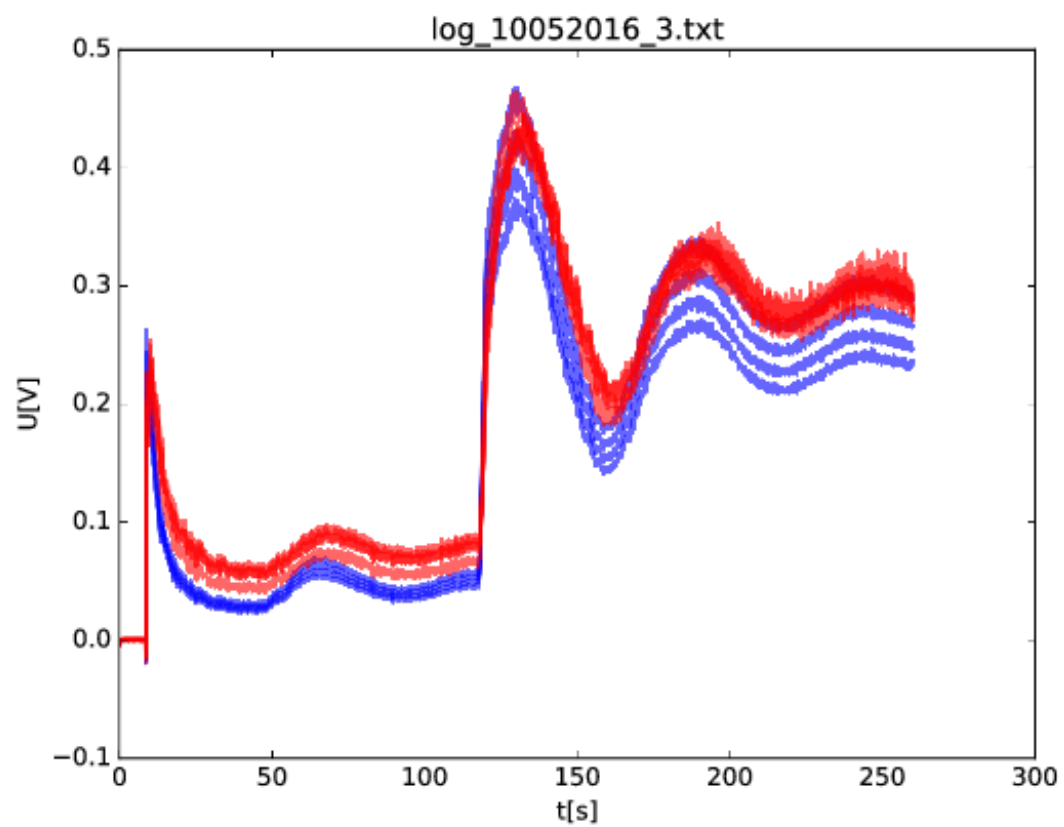


**Figure 5.7.:** feed add

## **6. Conclusion**

The conclusion is it works.

# **Appendix**

## A. Abbreviations

CFD	Computational Fluid Dynamics
PBR	Photobioreactor

## B. List of Figures

2.1. The inlet through which the water is fed back from the bottom of the reactor to the top . . . . .	11
3.1. equivalent circuit diagram . . . . .	15
3.2. electrode configuration . . . . .	15
3.3. Fisher Scientific™ Traceable™ Salinity Meter Pen [5] . . . . .	18
4.1. System Design . . . . .	20
4.3. A handmade sensor strip . . . . .	22
4.2. An electrode pair forming a sensor. . . . .	22
4.4. The sensor strip design to be implemented as flexible PCB. . . . .	23
4.5. A sensor strip manufactured by LEITON and assembled with cables and waterproofing. . . . .	23
4.6. Functional block diagram of ADG738 . . . . .	24
4.7. Timing diagram . . . . .	25
4.8. OpAmp . . . . .	26
4.9. After the switch, the capacitor discharges slowly. . . . .	27
4.10. The response immediately follows the switching event, but the AC signal is now unfiltered. . . . .	28
4.11. The assembled carrier boar with all parts mounted. . . . .	30
4.12. Data Format . . . . .	31
4.13. Embedded Software Flow Diagram . . . . .	32
4.14. OpenSalinity GUI . . . . .	33
4.15. Fixing the integer wrap of the time variable. . . . .	35

5.1.	A dimensioned drawing of the sensor grid made up by two strips placed next to each other, not drawn to scale and cut on the right side. It shows the sensor size of 10x11 mm, the horizontal distance between sensors of 50 mm and the vertical distance of 25 mm. . . . .	38
5.2.	The control volumes in blue have the same size as the sensor (black rectangle). At $t = 0$ the measurement starts and the first control volume is directly over the sensor. When the measurement ends at $t = \tau$ the control volumes have moved. The sensor is covered by a mix of the two volumes. . . . .	39
5.3.	The sensor strips are mounted to the bioreactor with electrical tape. Cables of 1 m length run towards the carrier board which is not in the frame. . . . .	41
5.4.	A laptop is used as host PC. A USB cable connects to the microcontroller on the carrier board, which is mounted on the side of the inlet basin. .	42
5.5.	noise . . . . .	43
5.6.	feed switch . . . . .	44
5.7.	feed add . . . . .	45

## C. List of Tables

2.1.	Requirements . . . . .	13
4.1.	BOM . . . . .	36

## D. Bibliography

- Commons, Creative (2016). Creative Commons Attribution-ShareAlike 3.0 Unported. 2016. URL: [https://creativecommons.org/licenses/by-sa/3.0/deed.en\\_US](https://creativecommons.org/licenses/by-sa/3.0/deed.en_US).
- Devices, Analog (2016). ADG738/ADG739 Data Sheet. 2016.
- Edwards, Ryan (2016). MinieC I2C eC interface. 2016. URL: <https://www.sparkyswidgets.com/portfolio-item/miniec-i2c-ec-interface>.
- fisherci (2016a). Fisher Scientific™ Traceable™ Conductivity, Resistivity, and TDS Meter. 2016. URL: <https://www.fishersci.com/shop/products/fisher-scientific-traceable-conductivity-resistivity-tds-meter/093262>.
- fisherci (2016b). Fisher Scientific™ Traceable™ Salinity Meter Pen. 2016. URL: <https://www.fishersci.com/shop/products/fisher-scientific-traceable-conductivity-tds-salinity-meter-pens-2/15078202>.
- Gevatter, HJ (2000). Automatisierungstechnik 1. Meß-und Regeltechnik. 2000.
- Tränkler, Hans-Rolf and Leonhard M Reindl (2015). Sensortechnik: Handbuch für Praxis und Wissenschaft. Springer-Verlag, 2015, p. 1152.